



Corrosion of Welded Carbon Steel Pipes in Oil Production Fields in Egypt



CrossMark

El-Morsy M.M.¹ and O.E. Abdel-Salam²¹Corrosion Department, Gulf of Suez Petroleum Company, Cairo, Egypt.²Chemical Engineering Department, Cairo University, Giza, Egypt.

IN oil production fields, corrosion of welded carbon steel pipes frequently occurs in areas near welds. Corrosion in other areas may take place at a lower frequency and with a lower detrimental effect. In this paper, a field survey is conducted of eight oil petroleum fields over a period of seven years. Testing of specimens of carbon steel welded joints is carried out under simulated conditions. This study investigates the predominated corrosion damage mechanisms in welded carbon steel pipes. It examines the critical factors triggering corrosion mechanisms and the techniques for corrosion monitoring and mitigation. Flow-induced corrosion and preferential weld corrosion were found to be the most effective mechanisms compared to pitting and microbiologically induced corrosion. Detrimental factors of corrosion mechanisms include flow rates and changes in process parameters of pH, fluid resistivity, and some anion concentrations. The corrosion mitigation was achieved by increasing the dosage of injected corrosion inhibitors.

Keywords: Preferential weld, Flow induced, Carbon steel, Oil.

Introduction

Corrosion in welded carbon steel pipes in oil production fields takes place in areas near welds at a high frequency and impact. Corrosion in other areas is possible but at a lower frequency and impact. Earlier scholars defined preferential weld corrosion and flow-induced corrosion as two corrosion mechanisms that take place in welded carbon steel pipes. However, these researchers did not deeply examine the characteristics of these mechanisms under functional flowing conditions in any of the industrial fields. Therefore, this paper aims to study these corrosion mechanisms in welded carbon steel pipes in oil production fields.

Two of the most frequently occurring types of corrosion of carbon steel pipes are the preferential weld corrosion and flow-induced corrosion. Pitting and stress corrosion cracking can also

exist in welded carbon steel piping. The Heat Affected Zone “HAZ” is the portion of the base metal that has not been wholly melted, but whose microstructure or mechanical properties have been altered by the heat of welding. The width of the heat-affected zone is a function of the heat input rate. Most plain carbon and low-alloy steels have a value of 5.9mm as a theoretical maximum HAZ width.

Preferential weld corrosion (PWC) is defined as the active corrosion mechanism of carbon steel weldments in corrosive environments. The variation in the microstructure of the welded zones is caused by the heat input results of the welding process. Each microstructure has different levels of corrosion resistance. This difference allows the formation of galvanic cells between different weldment's zones. In the case of welded piping, the liquid flowing film is the electrolyte, which is necessary to complete

*Corresponding author e-mail: Mazen.mahmoudam@yahoo.com

Received 6/11/2019; Accepted 14/1/2020

DOI: 10.21608/ejchem.2020.19176.2178

© 2020 National Information and Documentation Center (NIDOC)

the formation of galvanic cells of PWC. Liquid film thickness and conductivity are parameters determining resistance against corrosion current between anode (HAZ/ weld) and cathode (adjacent base metal). The conductivity of the liquid film is determined by the composition of the film in percentages of cations and anions. The polarity of the weld determines the effect of PWC. The overall galvanic PWC cells of a cathode weld are higher than those of an anode weld.

Flow-induced corrosion (FIC) is a mechanism by which an ordinarily protective oxide layer on a metal surface dissolves in fast flowing water. FIC is increased corrosion resulting from increased fluid turbulence intensity and mass transfer with fluid flow over a surface. FIC has been postulated to occur in carbon steel. FIC is distinguished from erosion corrosion because there is no impingement of particles, bubbles, or cavitation. FIC involves the dissolution of typically poorly soluble oxides by combined electrochemical, water chemistry and mass-transfer phenomena. Flow disturbances cause an increase in corrosion rate even when the flow velocity is not high. Examples for such disturbances occur at downstream of weld beads and pipefittings [1-17].

This study aims to fully investigating the true corrosion behavior of carbon steel pipes in oil production fields. A technical research and evaluation of the pipes is conducted under the actual service conditions.

The used welding in entire of this work is done by SMAW process. All tested welds are welded in workshop of oil field, where some of the tested welds are in practical pipe in actual oil fields and others are welded in also the workshop but they are tested in a lab. SMAW process is referred to "Shielded Metal Arc Welding". So, SMAW process is of arc welding types that are not usually involve pressure but may utilize a filler metal. The arc is a result from the crash between the work piece and the tip of the electrode.

SMAW is called Stick welding; or simply, it is called arc welding. It rules as the most commonly used type of welding. Its portable equipment is simple and cheap. It can be applied in windy conditions because the flux on the rod turns into slag that protects the weld from air. It can produce some high quality welds. Change from carbon steel to stainless steel is applicable by use of suitable sticks.

Power source is needed in SMAW; it should have adequate current rating and duty cycle, suitably sized electrical cables, an electrode holder, and a work piece-lead clamp. Utility-duty, single-phase alternating-current (AC) welding machines are the least expensive and can be used with small electrodes. Industrial-duty alternating / direct current (AC/DC) or DC power sources can be used with the greatest variety of electrodes.

The consumable electrode encloses some of consumable materials that act to provide arc stabilizers and vapors, which are necessary to displace air, metal and slag to protect, support, and insulate the hot weld metal. The latter action is needed to afford sufficient and accepted welding process. Example for consumable materials are silicate binders and powdered materials such as fluorides carbonates, oxides, metal alloys, and cellulose. The mixture of the said consumable materials is extruded around a wire core.

The ingredients in the coatings perform a number of functions. They stabilize the arc, thereby rendering excellent operation performance. They produce (1) shielding vapors, which displace air; (2) deoxidizers and other scavengers that purify the weld; and (3) slag, which provides a physical protection or "lid" over the hot weld metal.

The bare section of the electrode is clamped into an electrode holder, which, in turn, is connected to the power source by a cable. The work piece is connected to the other power source terminal. The arc is initiated by touching the tip of the electrode on the work piece and then withdrawing it slightly. The heat of the arc melts the base metal in the immediate area along with the electrode's metal core and covering. The molten base metal, the wire core, and any metal powders in the covering coalesce to form the weld [18,19].

The composition of arc welding process's rods can effect on corrosion rate; addition of noble metals (e.g. Ni, Cr, Mo, and Cu) to the weld consumable can control PWC; where some of them allows the weld metal to be cathode with respect to the adjacent pipe and HAZ. While, the over alloying of Ni or Ni-Cu can induce corrosion attack for HAZ; so the percentage of these additives shall be controlled. The addition of Ni and Mo shall be sensitive because both can cause detrimental effect in some cases; this effect is allowing of weld area to be anode with respect to HAZ and base metal. Silicon has also the same detrimental effect but in lower level [4, 20].

Corrosion mechanisms are one of damage mechanisms types that can affect any metal including weldments. Loss in thickness due to different corrosion mechanisms is one of damage mechanism in weldments; while other damage mechanisms types are found in the weldments. Examples for other damage mechanisms, which effect weldments particularly in HAZ, are loss of ductility and cracking.

The occurrence of one of corrosion mechanisms and probability to increase of its rate depend on many factors are :

- Weldment design and fabrication technique that might lead to high residual stresses
- Welding practice and sequence like to final surface finish, improper choice of filler metal and unbalancing of alloy compositions can cause certain precipitation reactions.
- Foreign components including moisture uncleanness, different chemicals' sorts including oxides, weld slag and spatter. Some of welding process provides protection against some sides of foreign components effect; as example, applying of shielding environment for molten and hot metal surfaces from reactive gases in the weld environment.
- Weld defects like to incomplete weld penetration or fusion, porosity, cracks.

The variations in above factors and in the welding processes parameters than acceptable limits allow occurrence of many of corrosion

mechanism; some of these mechanisms are preferential weld corrosion flow induced corrosion pitting corrosion and microbiologically influenced corrosion [3, 7, 21].

Field Statistical Analyses

The first field statistical analysis aims at defining the length of the area suffering high corrosion because of PWC, FIC, or both. This analysis is based on six case studies of different pipework systems in oil production fields. The material of construction of the entire piping systems is carbon steel grade B alloy. This is a commonly used material in the oil production field. The alloy's metal composition is described in Table 1; the analysis for the metal composition is in the reference [Ref: 3], while there is no mention for type of apparatus that was used for analysis. Ultrasonic (UT) examination is used to measure the wall thickness. The measured portions are the bottom half where corrosion occurs because of associated formation water. The water analysis for each case is presented in Table 2; the water analysis was done in specified Lab in the field using ICP (Inductively Coupled Plasma) apparatus.

Each of the piping system cases has a pipe diameter and flow condition, as demonstrated in Table 3. The cases are selected to provide a variety of operating flow conditions and pipe diameters. This variety gives evidence for results of the statistical field analysis.

TABLE 1. Metal composition for carbon steel grade B alloy [Ref: 3].

Element	C	Mn	P	S	Si	Cr	Cu	Mo	Ni	V	Fe
Max Comp. %	0.3	1.06	0.035	0.035	0.1	0.4	0.4	0.15	0.4	0.08	97.04

TABLE 2. Some ions concentration (10³ ppm) for corrosive water in analyzed cases.

	Na ⁺	K ⁺	Ca ⁺⁺	Mg ⁺⁺	Mn ⁺⁺	Cl ⁻	SO ₄ ⁻	HCO ₃ ⁻
Case 1	21	0.4	4	2	0.004	44	2	0.276
Case 2	18	0.4	4	2	0.012	40	3	0.294
Cases 3-5	30	0.6	16	4	0.005	86	1	0.422
Case 6	28	0.6	9	3	0.014	66	2	0.388

TABLE 3. Pipe diameter and flow conditions of each case.

Case	Case 1	Case 2	Case 3	Case 4	Case 5	Case 6
Diameter	10"	8"	16"	12"	8"	16"
Flow conditions	Normal	Stagnant	Normal	Normal	Altered among stagnant and normal conditions	Normal

The UT measurement for wall thickness of the six cases reveal the presence of thirty-six corroded areas. These areas have different values of the reduction in wall thickness that is an indirect measure of corrosion severity. The distance measured from the nearest weld is the main parameter in this analysis. The aim is to determine the length of the area affected by corrosion in the weld location. Examples for the thirty-six corroded areas are shown in Table 4. These examples are selected for being the highest corrosion rate in each case.

The second statistical analysis identifies the relationship between the flow rate and salinity of corrosive medium affecting the corrosion rate. This analysis covers recorded anomaly cases for failures and reduction in wall thicknesses over seven years at eight oil production fields. These fields are named F1, F2, ..., F8, respectively. Each field consists of separate relatively small production oil platforms and a gathering station that is a relatively larger platform. The gathering station contains a two-phase separator, which separates the associated free gases from the oil

and water (liquid phase). The liquid from the separator consists of a separate water phase and oil phase. The two-phase water-oil fluid is considered a bulk water phase that fills more than a half of the bottom of the pipework loop. This has created an electrolyte that facilitates corrosion in the metallic pipework and its components.

Each production field has variant values of liquid flow. And their variant characteristics of anion and cation water analysis results reflect the degrees of salinity, pH, and water conductivity. The details of water characteristics in each field is presented in Table 5, including the concentrations of Cl^- and SO_4^{2-} anions. The water analysis was done in specified Lab in the field using ICP (Inductively Coupled Plasma) apparatus.

The flow rate value represents the rate of liquid flowing out of each separator in each field. The gathering station has a different number of two phases separators. This value of flow rate is the one used in the statistical analysis. The value of the flow rate for each field is in presented in Table 6; these values are gotten from flow meters' readings in each field.

TABLE 4. Examples for corroded areas in the cases study of first statistical analysis.

Case Study	Thickness (mm)		Reduction in wall thickness %	Defect (mm)		Distance from Weld (mm)
	Max	Min		Width	Length	
1	8	3	63%	70	90	5
2	13	2.5	81%	60	150	0
3	11.5	3.5	70%	20	20	0
4	11.5	3.5	70%	40	40	70
5	13.5	4	70%	20	20	20
6	12.5	3	76%	22	40	5

TABLE 5. Water characteristics of each field: values for ions and TDS are in ppm units.

	F1	F2	F3	F4	F5	F6	F7	F8
$\text{Cl}^- * 10^3$	99	82	112	105	151	75	48	86
SO_4^{2-}	180	660	240	1,050	540	3,100	2,000	2,133
$\text{TDS} * 10^3$	159	134	177	171	238	125	80	141
pH	5.55	6.09	5.36	5.83	5.64	6.14	6.58	6.27
Re ($\Omega \cdot \text{m}$)	0.031	0.039	0.029	0.029	0.022	0.042	0.061	0.036

TABLE 6. Value for field's flow rate (Barrel (BBL) per Day).

F1	F2	F3	F4	F5	F6	F7	F8
28,000	12,000	7,600	7,500	3,000	28,500	10,000	25,000

Numbers of recorded anomaly cases involving reduction in wall thickness of previously stated pipework loop is listed in Table 7. The anomaly case is defined as the case where certain pipework has localized corroded areas. These areas make the pipework unfit to withstand the interior operating pressure.

The localized corroded areas are measured by Ultrasonic (UT) examination. Fig. 1 shows an example of an anomaly case in a UT report. A drawing of a spool joint and measurements of the localized corroded areas in this spool are shown.

The third analysis was conducted to determine effects of Cl^- ions, SO_4^{2-} ions, and pH on anomaly cases in each field. In this analysis, the number of anomaly cases is calculated by determining failure per year "FPY" term. FPY is equal to the number of anomaly cases divided by number of years when these anomaly cases took place. The field "F1" is replaced by two names "F1C" and "F1P" for two sub-periods. These periods represent the first five years and the latter two years. Replacement of "F1" was necessary because of changes in the characteristics of the oil field in the two cited sub-periods. Accordingly, the number of fields became nine.

Experimental Work

The first experiment determines suitability of corrosion coupon technique for corrosion monitoring in oil fields suffering high localized corrosion rates. The experiment is built on an approximate simulation of the actual exposure stagnant condition in the oil production field. Carbon steel pipes are used to get coupons that are used in the experiment. Cold cutting of natural edged pipes is used to simulate the effect of edging on corrosion behavior. Stagnant condition determines corrosive medium properties of pH and conductivity and their effect on corrosion excluding effects of the flow. Moreover, the experiment aims to determine the severity of water flow in field F1 that has the highest recorded anomaly cases as seen in Table 7. Another water corrosive medium was obtained from a source in an oil production facility. The said source is arbitrarily denoted by symbol "S1". Seawater was also used in this experiment and is arbitrarily denoted by symbol "S2". The concentrations of some ions and properties of the three samples are listed in Table 8.

TABLE 7. Numbers of recorded anomaly cases in each field through seven years.

F1	F2	F3	F4	F5	F6	F7	F8
61	14	1	11	6	16	7	7

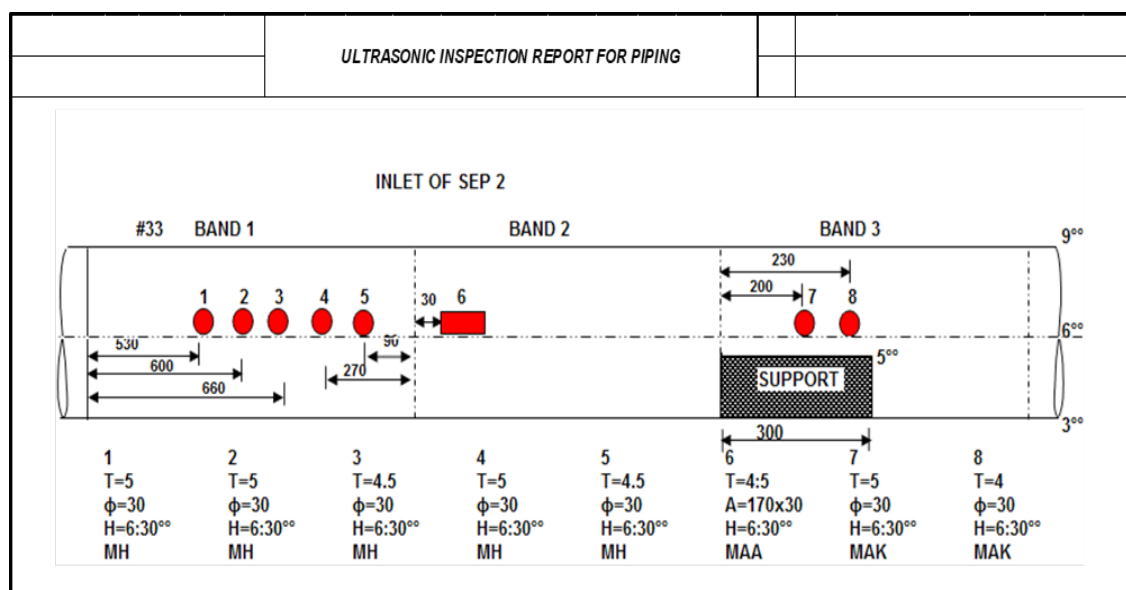


Fig. 1. UT Report for Spool Joint Locations and Measurements for Localized Corroded Areas Numbered 1 – 8.

Two standard edged carbon steel grade B pipes with 6" diameters are used. The two pipes were welded using the approved welding procedure (WPS) of a workshop in oil field F1. Shilled metal arc welding (SMAW) is used for welding. Radiography examination is conducted on the two welded pipes to verify acceptance and soundness of the deposited welding. Ultrasonic examination is conducted on the pipe to confirm the absence of any localized or general corrosion. Six coupons are cut from the constructed pipe. The photos

in Fig. 2 represent the pipe after cutting the six coupons. Three coupons are cut from the welded area to include a weld. The other three coupons are cut from the metal base that is relatively far from the welded area. The six coupons are immersed in the three corrosive mediums F1, S1, and S2 as shown in Fig. 3. Each corrosive water medium has one immersed coupon from the welded area and another from the metal base. The characteristics of each coupon are listed in Table 9.

TABLE 8. Water characteristics for corrosive mediums in the first experiment: values of ions and TDS in ppm units.

	F1	S1	S2
Fe ⁺⁺	193	128	0
CL ⁻	99,152	82,278	24,799
SO ₄ ⁻	180	1,150	3,050
TDS	158,863	133,998	44,509
pH	5.55	5.93	6.39
Cond. S/cm	320,000	272,040	91,743



Fig. 2. Constructed pipe and its coupons.

Fig. 3. Coupons in their plastic containers.

TABLE 9. Number and dimensions of the immersed six coupons.

Coupon No.	Corrosive water medium	Type of coupon	Dimensions of coupon (inch) with 0.28" thickness			Original weight (gm)
			Length	width	Exposed area	
1	S2	Weld	2.05	1.81	9.8	141.125
2		Base	2.95	1.57	12.2	172.7132
3	S1	Base	2.32	2.17	12.9	122.2138
4		Weld	2.20	2.17	12.3	148.574
5	F1	Base	3.03	2.01	15.4	178.702
6		Weld	3.11	1.93	15.3	186.7565

Weight loss and Fe^{++} content techniques are used to monitor and measure the corrosion rate. The experimental period lasted for 125 days. The coupons are immersed for 75 days. Then, they are weighed after washing them with xylene and acids. Washing removed any traces of deposited hydrocarbons formed during immersion period or any solid desposits caused by corrosion. Coupons were then re-immersed for an additional 50 days. Weights of the final coupons were calculated at the end of the 50 days. At the end of the experiment, the water samples were re-analyzed to determine the concentration of existing Fe^{++} . The analysis was done by determining the amount of Fe^{++} per million (ppm) using ICP (inductively coupled plasma) equipment. Fe^{++} content represents the difference between values of the analyzed water samples before and after the experiment.

The second experiment verifies the presence of an anode area adjacent to the weld. The existence of a higher localized corrosion rate compared to the general corrosion rate was verified. Potential survey technique applied to the pipe's external surface used a highly sensitive voltammeter to measure corrosion current in microampere units. Two carbon steel grade 35 pipes with a 6cm length each were used. The metal composition of carbon steel grade 35 alloy is listed in Table 10. SMAW is used for welding with an approved WPS.

Condition of stagnant flow is implemented by filling the 1" welded carbon steel pipe with

corrosive water medium S2 (seawater). Then, the pipe ends are sealed and set under the cited conditions for 60 days, as shown in Fig. 4.

Potential survey technique is applied by setting one probe of the highly sensitive voltammeter adjacent to the weld. The other probe is set at different distances from the weld as shown in Fig. 5. The voltammeter is set on the DC system and microampere scale. The aim is to measure corrosion current between separately formed anode and cathode areas in the welded pipe. Some measurements are done by setting the positive probe at the weld. Other ones are done by setting the negative probe at the weld to compare polarity of the measured current.

For corrosion mitigation, additional experimental work was done. The corrosion inhibitor dosage is doubled in field F1. The corrosion rate and FPY are observed for an additional two years other than the mentioned seven-year period of field survey.

Results and Discussion

A statistical analysis was conducted for the 36 corroded areas in the first field. The corroded areas were identified in in-service pipes in the field using Ultrasonic (UT) flaw detector device with commercial type called "OLYMPUS" and model number "EPOCH 600". Figure 6 shows an example for the process for using of the cited UT device to locate a corroded area.

TABLE 10. Metal composition of carbon steel grade 35 alloy [Ref: 3].

Element	C	Mn	P	S	Si	Cr	Cu	Ni	Fe
Max Comp. %	0.4	0.8	< 0.035	< 0.04	0.37	< 0.25	< 0.3	< 0.3	> 97.505



Fig. 4. Two pipe pieces after welding and filling with corrosive water S2 (seawater).

The statistical analysis revealed that the area with the highest corrosion rate has a longitudinal distance of 150mm from the weld. The analysis is done by dividing the corroded areas into groups (A, B, C & D) and subgroups. It is based on distance between corroded area and nearest weld between joints of the pipe (see Table 11). Table 11 includes counts of corroded regions located in each subgroup of the cited main groups. The largest count is in group A.

Areas with the highest reduction in wall thickness are located at distances of less than 150mm from girth weld (see Table 4). The corroded area in case (2) in Table 4 is located at zero distance from the weld. Flow condition is stagnant in this corrosion case because of the PWC mechanism.

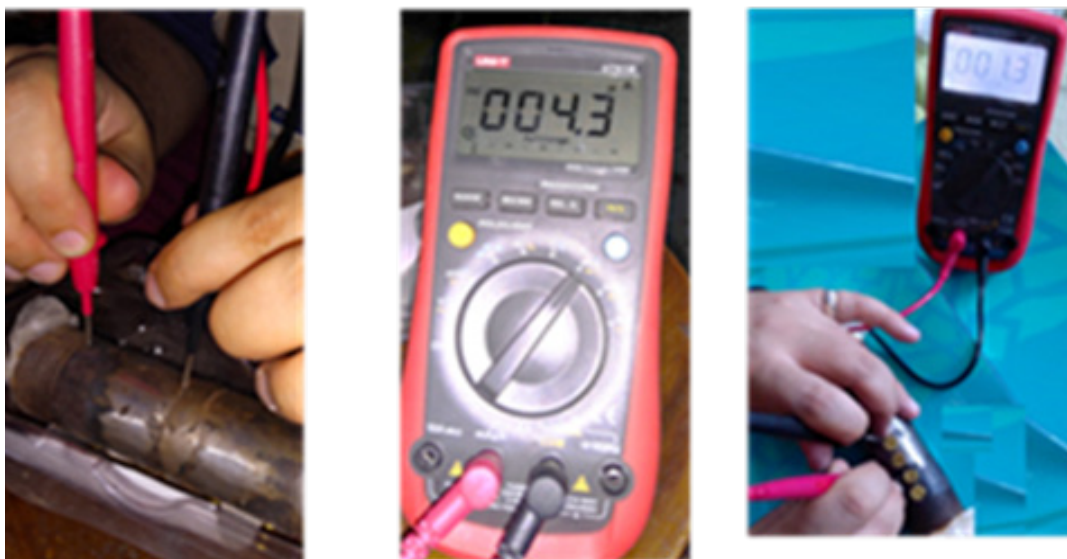


Fig. 5. Potential Survey on the External Pipe Surface Using Voltammeter.



Fig. 6. Photo for example of using of OLYMPUS UT device to locate corroded area.

TABLE 11. Counts of Corroded Areas in Each Group and Their Subgroups.

Actual Distance (mm) from weld		Sub-Class	Sub-class Count	Class	Count
from	to				
0	0	A1	6		
5	20	A2	7	A	19
50	80	A3	2		
150	300	A4	4		
420	500	B1	4	B	6
550	600	B2	2		
1210	1380	C1	2		
1940	1960	C2	4	C	11
2200	3700	C3	5		

The results of the second field statistical analysis that are in Table 7. It demonstrates the relationship between the severity of corrosion in the liquid medium and the flow rate. The highest count of the recorded anomaly cases is in field "F-1". As per Tables 5 and 6, the said field has relatively lower water resistivity and high flow rate. These are essential factors in corrosion management of the oil production facilities. In this concurrent high flow rate and low water resistivity, there is an expectation for the high corrosion rate. This was found in 61 recorded anomaly cases of field "F-1" with the highest recorded anomaly cases compared to other fields. Absence of low resistivity water conditions, as in field "F-8" resulted in only 7 recorded anomaly cases in 7 years. Resistivity of field "F-5" is lower than the resistivity of field "F-1". The count of recorded anomaly cases of field "F-5" is relatively smaller because of low flow rate in this field.

The nine fields included in the third field statistical analysis are divided according to flow rate. The values of the flow rate range from low to high flow rate regions. The low flow rate region is for fields with a flow rate of less than 1,000 BBLD. And, the high flow rate region is for fields with a flow rate of more than this value. The data for water chemistry, including Cl^- and SO_4^{2-} concentration, are obtained from Table 5. The recorded number of failure cases are divided by the number of years to give a rate of failure (FPY). "FPY" represents failure per year. FPY and $\text{Cl}/\text{SO}_4^{2-}$ ratios per field are listed in Tables 12 and 13, representing low and high flow rate regions, respectively. The data in Tables 12 and 13 are arranged in a descending order according to FPY value. The resistivity values were measured

by TDS meter device with market name (Mettler Toledo) and the pH values were measured using pH meter device.

In high flow rate cases, results of fields "F7" and "F6" are discarded. This is because they have the same $\text{Cl}^- / \text{SO}_4^{2-}$ ratio with different FPY. In addition, the value of FPY in "F7" is the same as that in "F8". Disruption in "F7" and "F6 data" might result from increased failure rate during some period owing to abnormal operations. Therefore, the considered data for analysis was restricted to "F8", "F2", "F1P", and "F1C". In low flow rate regions, there is an inverse relation between $\text{Cl}^- / \text{SO}_4^{2-}$ ratio and FPY. In the high flow rate regions, this relation is direct as shown in Fig. 7. The pH has an inverse relation to FPY in the low flow rate region and a direct relation in the high flow rate region.

The results of the first experiment are presented in Table 14. The values for Fe^{++} are gotten using ICP apparatus; while the weight of coupons are measured using high sensitive digital balancer in Lab. The welded coupons compared to the base metal coupon have lower corrosion rates. These rates are measured in the overall experiment period (125 days) and the first period of the experiment (75 days). The net dissolved iron of the welded coupons is lower than the net dissolved iron of the base metal coupon. Despite a considerable percentage of recorded anomaly cases in "F-1", results of the welded coupons indicate a lower corrosion rate. The corroded areas near the weld are caused by PWC. Confusing results of the later experiment result from the weight loss and Fe^{++} content techniques based on general corrosion. Failures caused by PWC, FIC or both are localized. These failures result in

lower weight loss despite deep loss in thickness owing to small anode area. Therefore, the used techniques in the said experiment are misleading of the actual corrosion rate in the field. Therefore,

the monitoring technique is selected based on the damage mode of the credible corrosion mechanisms.

TABLE 12. Low flow rate field cases in descending arrangement according to FPY.

Field	Flow Rate BBLD*10 ⁻³	pH	Resistivity * 10 ² (Ωm)	Cl ⁻ ppm	SO ₄ ²⁻ ppm	FPY	Cl ⁻ / SO ₄ ²⁻
F3	7.6	5.36	29	112,024	240	0.14	467
F5	3	5.64	22	151,165	540	0.86	280
F4	7.5	5.83	29	105,900	1050	1.57	101

TABLE 13. High flow rate field cases in descending arrangement according to FPY.

Field	Flow Rate BBLD*10 ⁻³	pH	Resistivity *10 ² (Ωm)	Cl ⁻ ppm	SO ₄ ²⁻ ppm	FPY	Cl ⁻ / SO ₄ ²⁻
F7	10	6.58	61	47905	2000	1	24
F6	28.5	6.14	42	75,320	3100	2.29	24
F8	25	6.27	36	86,366	2133	1	40
F2	12	6.09	39	82365	660	2	125
F1P	21	5.9	34	93,983	300	2.8	313
F1C	28	5.5	31	99,152	180	23.5	551

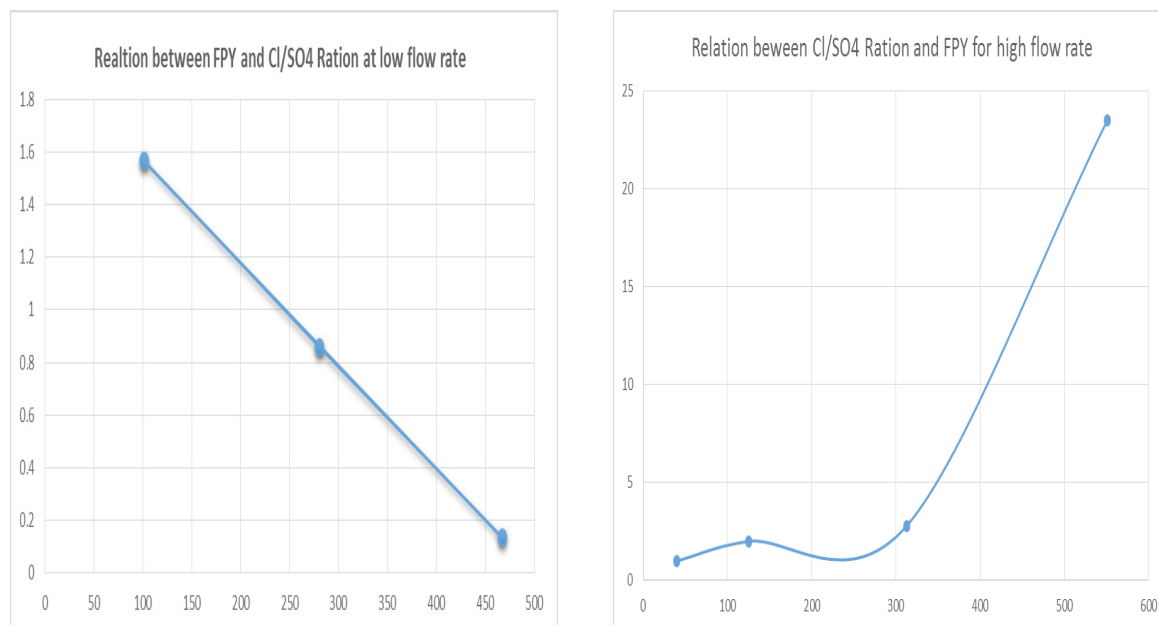


Fig. 7. Charts for the relation between Cl⁻ / SO₄²⁻ ratio and FPY.

The potential survey results of the measured corrosion current in the second experiment are shown in Table 15. The change in the polarity in current measurements are demonstrated in Table 14. Here the area at the weld is the anode connecting other pipe portions, and it is relatively far from the weld. The anode area at the weld causes the activation of PWC. The maximum measured current can be converted into a corrosion rate in mpy units using Faraday equation. This is done by calculating surface area of the pipe where the current passes and density of the carbon steel pipe. The calculated rate is found to be 4 mpy that is the rate for localized corrosion resulting from PWC. This rate is higher than the

1 mpy corrosion rate in the general corrosion case of seawater in the first experiment. Therefore, the rate of localized corrosion is higher than general corrosion. This proves unsuitability of corrosion coupon technique as a corrosion monitoring technique in localized corrosion as in the case of PWC.

For corrosion mitigation, doubling of the corrosion inhibitor gives zero FPY in the two additional years. This result might refer to the loss in corrosion inhibitor film because of flow effect. This would require continuous maintenance to obtain the required corrosion inhibitor film thickness.

TABLE 14. Weight loss and Fe⁺⁺ content results of coupons in first experiment.

Test media	Type of Coupon	Weight Loss Corrosion Rate (mpy)		Fe ⁺⁺ Content Analysis (ppm)		
		125 Days	75 Days	Original	after 125	Net Dissolved
S-2	Weld	0.72	0.91	0	318	318
	Base	0.81	0.96	0	316	316
S-1	Base	0.05	0.26	128	371	243
	Weld	0.04	0.18	128	319	191
F-1	Base	1.62	1.12	227	1006.6	779.6
	Weld	1.28	0.82	227	676.2	449.2

TABLE 15. Potential survey results for second experiment.

Probe adjacent to weld	Distance between probes (mm)	Location of probes on pipe	Current μ Amp	Polarity of current
Negative	5	Top	0.2	+ Ve
	300	Top	1.3	
	300	Middle	0.8	
	600	Bottom	4.3	
Positive	600	Top	-2.5	- Ve
	5	Top	-0.3	
	600	Bottom	-3.8	

Conclusion

The portion with a high corrosion rate is adjusted to a girth weld between pipe joints, with the longitudinal length of 50mm to 150mm. There may be other areas with high corrosion rate in the welded carbon steel pipes. It is important to note that flow rate must be considered in corrosion management. For a concurrent high flow rate and low resistivity, a high corrosion rate is expected. In this case, the dosage of corrosion inhibitor should be doubled. This is to make up for losses in corrosion inhibitor due to strong shear force of the high flow rate. In low flow rate regions, there is an inverse relation between Cl^- / SO_4^{2-} ratio and FPY. In high flow rate regions, this relation is direct. Moreover, the pH has an inverse relationship with FPY in low flow rate regions and a direct relation in high flow rate regions. Finally, it is noteworthy to mention that the localized corrosion rate is higher than the general corrosion rate. Therefore, the use of the corrosion coupons monitoring technique is not suitable in the case where localized corrosion is predominant. One of the appropriate corrosion monitoring techniques occurs in the case where localized corrosion is predominant is a potential survey.

References

1. Callister W.D., "Materials Science and Engineering: an Introduction in Chemical Thermodynamics for Metals and Materials", 2007
2. Smith, William F.; Hashemi, Javad, "Foundations of Materials Science and Engineering", fourth edition, McGraw-Hill, New York, NY, USA, 2006
3. Shackelford, James, "Introduction to Materials Science for Engineers, 7th Edition, Upper Saddle River, ISBN 0-13-601260-4, 2009
4. D. Gandy, Carbon Steel Handbook, Electric Power Research Institute, EPRI, California, USA, 2007
5. Pierre R. Roberge, Handbook of Corrosion Engineering, Chapter 8 – Material Selection, McGraw-Hill Book Company, New York, NY, USA, 1999
6. R. E. Smallman, R. J. Bishop, Modern Physical Metallurgy and Materials Engineering, Sixth Edition, Butterworth-Heinemann, Johannesburg, 1999
7. Cynthia L. Jenney, Annette O'Brien. Welding Handbook, Volume 1, welding science and technology, Ninth Edition, American Welding Society, 550 N.W. LeJeune Road, Miami, 2001
8. Callister, D. William, "Fundamentals of Materials Science and Engineering," John Wiley & Sons, Inc. Danvers, 2005
9. Nathalie Ochoa, "CO₂ Corrosion Resistance of Carbon Steel in Relation with Microstructure Changes", Materials Chemistry and Physics, Vol.156., p.198-205, 2015
10. Tsiourva D., Dimaratos L.I., "Corrosion Behavior of Shipbuilding High Strength Steel Welds Empolying Electrochemical Methods", Maritime Transportaion and Exploitation of Ocean and Coastal Resources, Vol. 1, p. 543-548, 2005
11. David Queen, Chi-Ming Lee, "Guidelines for the Prevention, Control and Monitoring of Preferential Weld Corrosion of Ferritic Steels in Wet Hydrocarbon Production Systems Containing CO₂", 1st International Symposium on Oilfield Corrosion, Aberdeen, UK, 2004
12. Uhlig's Corrosion Handbook, 2nd edition, "Chapter 14 - Flow Induced Corrosion", Winston Revie R., John Wiley & Sons, Inc. New York / Chi-Chester / Weinheim / Brisbane / Singapore / Toronto.
13. Palo Alto, "Flow-Associated Corrosion in Power Plants", Report TR-106611-R1, Electric Power Research Institute, California, Jul 1998
14. Alireza Bahadori, "Oil and Gas Pipelines and Piping Systems: Design, Construction, Management, and inspection", 1st Edition, Gulf Professional Publishing, ISBN 9780128037775, 2016.
15. Barker R., Hu X., Neville A., Cushnaghan S., "Inhibition of Flow-Induced Corrosion and Erosion-Corrosion for Carbon Steel Pipe Work from an Offshore Oil and Gas Facility", Corrosion-Vol. 69, No. 2, NACE International, 2012.
16. Richard Barker, Xining Hu, Anne Neville, "Assessment of Preferential Weld Corrosion of Carbon Steel Pipework in CO₂ Saturated Flow Induced Corrosion Environments", NACE, Conference, Publications Division, 1440 South Creek Drive, Houston, Texas, 2012.
17. Yong X. Y., Zhang Y.Q., Li D. L., Wang J.D., "Effect of Near-Wall Hydrodynamic Parameters on Flow Induced Corrosion", Corrosion Science and Protection Technology, pp.245-250, 2011.
18. D. L. Olson, T. A. Siewert, ASM Metal Hand Book, Volume 6, Welding, Brazing, and Soldering,

-
- Thomas W. Eagar, Massachusetts Institute of Technology, 1993
19. J. E. Meyer, D. W. Diehl, elite, International piping code, ASME Code for Pressure Piping, B31, The American Society of Mechanical Engineers, Two Park Avenue, New York, NY 10016-5990, 2016
20. E. Bülent, A. Aysegül, Corrosion Behavior on the Types of Weld Joints, METAL, 2006
21. J. R. Davis. Corrosion of Weldments, The Material Information Society, USA, ISBN-10: 0-87170-841-8.